Metal–Organic Frameworks

DOI: 10.1002/anie.201003900

Urothermal Synthesis of Crystalline Porous Materials**

*Jian Zhang, Julia T. Bu, Shumei Chen, Tao Wu, Shoutian Zheng, Yigang Chen, Ruben A. Nieto, Pingyun Feng, and Xianhui Bu**

Intensive research in the past several decades has resulted in the synthesis of porous materials with diverse chemical compositions and framework topologies.[1] However, the search for new porous materials continues to be a highly active field because of their potential applications in emerging areas, such as gas storage,[2] CO_2 capture,[3] and catalysis.[4]

Porous materials are usually synthesized at relatively low temperatures ($<200\,^{\circ}C$), which necessitates the use of solvents to promote the diffusivity of reactants and to grow crystals of suitable sizes. In fact, solvents have played vital roles in the development of different families of porous materials. For example, inorganic porous materials such as zeolites are often synthesized using the hydrothermal method, even though non-aqueous synthesis has also been explored.[5] On the other hand, recently developed metal–organic frameworks (MOFs) often rely on the use of organic solvents such as DMF in a process called solvothermal synthesis. It is worth noting that solvothermal synthesis is an overly broad concept, covering solvents with dramatically different structures and properties. As such, it generally conjures up little correlation between solvents used and structural features or properties of materials prepared in them. With the recent advance in the understanding of correlations between structures and properties, it has become increasingly desirable to design synthetic methods to target specific structural features and physical or chemical properties.

Herein, we explore a versatile method (which we denote as urothermal synthesis) that is based on the use of various urea derivatives as solvents. One highly useful feature of urothermal synthesis is the reversible binding of urea derivatives to metal sites, which allows them to competitively bond to framework metal sites and yet in many cases they can be easily removed after crystallization to generate both porosity and open metal sites. The competition for coordination to metal sites among urea derivatives and against other solvents such as DMF or DEF is an interesting aspect of this synthetic process and can also be utilized to provide additional structural control.

Prior to this work, urea and urea derivatives were rarely used as solvents for the synthesis of MOFs. However, as a well-known component in deep eutectic solvents, urea and urea derivatives have contributed to the ionothermal synthesis of interesting porous materials, sometimes through decomposition to generate amine templates.[6]

The large variety of urea derivatives, together with various organic crosslinking ligands and metal ions create numerous synthetic possibilities, as shown by many new materials prepared in this work (Tables 1; Supporting Information, S1). These materials comprise various organic ligands (Supporting Information, Scheme S1), many metal ions, and five symmetrical urea derivatives (two with N–H groups and three without; Scheme 1). For comparative purposes, one cyclic and two acyclic amide solvents, namely DMF, DEF, and 2-pyrrolidinone (pyrol), were also studied.

Table 1: A summary of the materials prepared herein.[a]

Compound	Space group	Additional roles of solvents
$[Y_2(bdc)_3(e\text{-}urea)_2(H_2O)_2]$ (**1**)	$P\bar{1}$	mixed pendant ligand
$[Y_2(bdc)_3(e\text{-}urea)_4]$ (**2**)	$P\bar{1}$	pendant ligand
$[Y_2(bdc)_3(e\text{-}urea)_2(p\text{-}murea)_2]$ (**3**)	$P\bar{1}$	mixed pendant ligand
$[Y_2(bdc)_3(e\text{-}urea)_2(DEF)_2]$ (**4**)	$P\bar{1}$	mixed pendant ligand
$[Y_2(bdc)_3(e\text{-}urea)_2(DMF)_2]$ (**5**)	$P\bar{1}$	mixed pendant ligand
$[Y_2(bdc)_3(DEF)_2]$ (**6**)	$C2/c$	pendant ligand
$[Y_2(bdc)_3(p\text{-}urea)_2]$ (**7**)	$P2_1/n$	pendant ligand
$[Y_2(bdc)_3(pyrol)_2]$ (**8**)	$P\bar{1}$	pendant ligand
$[Co_3(bdc)_3]\cdot(tm\text{-}urea)_x$ (URO-44)	$C2/c$	template
$[Cd_3(bdc)_3(H_2O)_2]\cdot(tm\text{-}urea)_x$ (URO-45)	$C2/c$	template
[Cd(1,3-bdc)(e-urea)] (URO-110)	$P2_12_12_1$	pendant ligand
$[Zn_4(OH)_2(1,2,4\text{-}btc)_2(H_2O)]\cdot$ (p-murea) (URO-123)	$P2_12_12_1$	template
$[Yb_3O(thb)_3(p\text{-}murea)_3]\cdot(NO_3)$ (URO-160)	$P31c$	pendant ligand
$[Cd(thb)(en)_{1/2}(e\text{-}urea)]\cdot$(e-urea) (URO-162)	$Pnma$	pendant and template
$[Cu_4I_4(L1)_4]$ (URO-502)	$C2$	reactant in in situ ligand formation
$[Li_2(tza)_2(e\text{-}murea)_{1.5}]$ (URO-511)	$P2_12_12$	pendant ligand

[a] For a more complete list of structures with crystallographic data, see the Supporting Information, Table S1, and for structural diagrams of crosslinking ligands, see Scheme S1.

[*] Dr. J. Zhang, Dr. S. Chen, Dr. S. Zheng, Y. Chen, R. A. Nieto, Prof. Dr. X. Bu
Department of Chemistry and Biochemistry
California State University, Long Beach, CA 90840 (USA)
Fax: (+1) 562-985-8557
E-mail: xbu@csulb.edu

Dr. J. Zhang
Fujian Institute of Research on the Structure of Matter
Chinese Academy of Sciences
Fuzhou 350002 (China)

J. T. Bu, T. Wu, Prof. Dr. P. Feng
Department of Chemistry
University of California Riverside (USA)

[**] We thank the NSF (X.B. DMR-0846958, P.F. CHEM-0809335), the DOE (P.F. DE-SC0002235), and the Research Corporation (X.B. CC6593) for support of this work. X.B. is a Henry Dreyfus Teacher Scholar. J.T.B. is a research intern from J. W. North High School.

Supporting information for this article is available on the WWW under http://dx.doi.org/10.1002/anie.201003900.

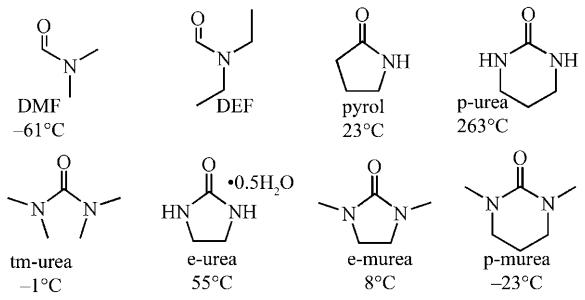

Scheme 1. The solvents used for synthesis. Values shown are melting points. DMF = dimethylformamide, DEF = diethylformamide, pyrol = 2-pyrrolidinone, tm-urea = tetramethylurea, e-urea = ethyleneurea, e-murea = 1,3-dimethyl-2-imidazolidinone, p-urea = propyleneurea, p-murea = 1,3-dimethylpropyleneurea.

These new structures reveal that the major interaction between urea derivatives and framework metal sites is the coordinate interaction between the carbonyl oxygen and metal ions (that is, −C=O−M), which is supplemented in some cases by a H-bonding interaction between N−H-containing urea derivatives and the oxygen of the carboxyl group. Some urea derivatives, such as tm-urea, e-murea, and p-murea (Scheme 1), have no N−H groups and therefore can not form N−H···O H-bonds. As shown below, the formation of H-bonding is one of the factors that affect the bonding affinity of urea derivatives to the framework metal sites.

Compounds **1** to **5**, based on the Y-bdc (bdc = 1,4-benzene-dicarboxylate) system, provide an excellent illustration of the roles of urea derivatives, especially the competitive bonding nature of different urea derivatives in relation to common solvents such as DEF. Even though Y^{3+} sites in as-synthesized crystals in **1**–**5** are eight-coordinate (two of which are two solvent molecules and are potential open-metal sites Supporting Information, Figure S1), **1**–**5** exhibit the same 4-connected moganite (denoted: mog) topology by reducing the Y^{3+} sites as 4-connected nodes (Figure 1 a,b). The difference among **1**–**5** is in the type of the pendent ligand attached to the framework (Supporting Information, Figure S1). Therefore, compounds **1**–**5** make it possible to probe ligand affinity to metal sites by keeping other structural features the same.

Compound **2**, made by using only e-urea hemihydrate as the solvent, illustrates dual interactions (−C=O−M and N−H···O) between urea derivatives and the framework. In **2**, two crystallographic independent e-urea ligands are coordinated to one Y^{3+} site and are situated inside the rectangular channel along the *a* axis (Figure 1 b). Each e-urea ligand forms one N−H···O H-bond with one carboxylate oxygen atom of the framework; the N···O distances are 2.769 Å and 2.990 Å, respectively, suggesting different H-bonding strengths. The e-urea associated with the weaker H-bond can be replaced by competing solvent molecules when the synthesis is performed in a mixed solvent, leading to the synthesis of **3** to **5**.

Compounds **3**–**5**, prepared from a mixed solvent system, allow us to compare the bonding affinity of different solvent molecules to the metal sites. Thus, the different combination of various solvents, e-urea with p-murea (**3**), e-urea with DEF

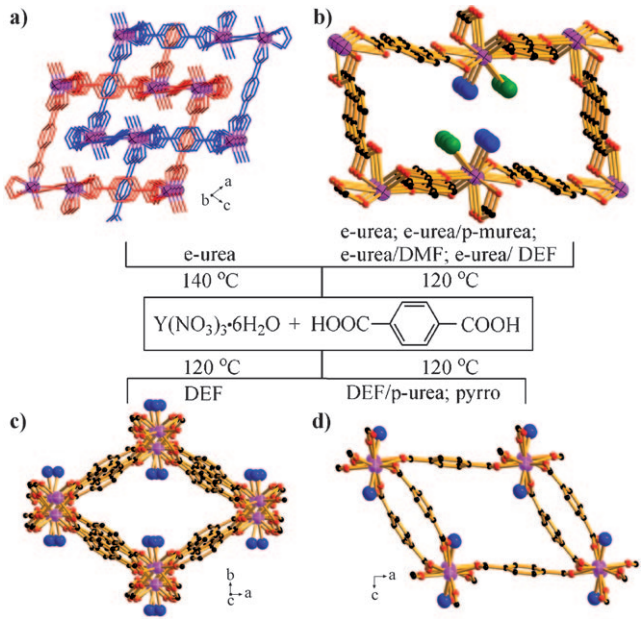

Figure 1. Four different framework types obtained from the self-assembly of $Y(NO_3)_3{\cdot}6H_2O$ and H_2bdc under different solvent conditions or temperatures. a) twofold interpenetrating mog-type framework in **1**; b) non-interpenetrating mog-type framework in **2**–**5**; c) (4,6)-connected framework in **6**; and d) (4,6)-connected framework in **7** or **8**. C black, O red, M pink; solvent molecules are shown as large blue and green spheres (potential open metal sites).

(**4**), and e-urea with DMF (**5**), leads to three framework structures (**3**–**5**) that are similar to **2**. However, both types of solvent molecules were incorporated as the pendent ligands. Half of the e-urea ligands in **2**, which have weaker H-bonds to the framework, are replaced by p-murea in **3**, DEF in **4**, and DMF in **5**, respectively (Supporting Information, Figure S1).

To further probe the bonding affinity, we also explored a three-component solvent system. In the case of e-urea/p-murea/DEF, **4** (instead of **3**) containing e-urea and DEF is formed. This synthesis shows that as far as the moganite topology is concerned, p-murea has a weaker affinity than e-urea and DEF. In **1**–**5**, the consistent formation of the mog-type frameworks is most likely dictated by the strong structure-directing role of e-urea through its combined −C=O−M and N−H···O interactions.

The difference between **1** and **2** shows the effects of reaction temperature and ligand size. By using the same reaction condition as **2**, except with an increase of the temperature from 120 to 140 °C, half of e-urea molecules in **2** are replaced by H_2O, leading to the formation of **1**. Even though **1** has the same mog topology as **2**–**4**, it has twofold interpenetration (Figure 1 a), which is most likely caused by small size of H_2O. This suggests that the twofold interpenetration in **1** is eliminated by replacing H_2O with larger solvent molecules, such as e-urea in **2**, p-murea in **3**, DEF in **4**, and DMF in **5**.

What will happen if e-urea, which favors the mog topology, is not used? Again, we focus on the Y-bdc system so that the solvent effect can be highlighted. Reactions between Y^{3+} ions and bdc in three solvent systems (DEF; DEF with

p-urea; and pyrol) generate three new structures (**6**–**8**) in which the Y^{3+} ions are bridged by carboxylate groups of bdc ligands into chains (Supporting Information, Figure S1 f–h) that are further crosslinked by benzene rings of the bdc ligands to generate the 3D framework (Figure 1 c,d). The solvent molecule in **6**–**8** is attached to Y^{3+} to complete its coordination geometry (Figure S1 f–h). Two different (4,6)-connected topologies were observed. In **6**, the distribution of solvent molecules (DEF) along the Y-BDC chain follows the UUDDUUDD… pattern (U = up, D = down), resulting in a (4,6)-connected trinodal net. In **7** (p-urea) and **8** (pyrol), the UDUDUD… pattern is observed, leading to another type of net.

The synthesis of p-urea-containing **7** from the mixed DEF and p-urea solvent further highlights the competitive bonding of ligands to the framework and confirms the significance of integrated metal–ligand and H-bonding interactions in enhancing the affinity of N−H-containing urea derivatives to the framework. When used alone, DEF is readily incorporated into **6**. However, when p-urea is used together with DEF, compound **7** which contains only p-urea is formed, even though the molar ratio of 5:1 between DEF and p-urea in the synthesis mixture is in favor of DEF.

It is also of interest to compare **2** and **8**, which are made from e-urea and pyrol, respectively. These two ligands have the similar size and shape, except that e-urea has an N−H group on both sides of −C=O group, whereas pyrol has an N−H group at only one side. Such a difference is, however, sufficient to generate two different framework topologies.

The urothermal synthesis shown above for the Y-bdc system can be extended to many metal ions including lanthanides (Ln), transition metals, and even alkali and alkaline-earth metals, thus demonstrating the versatility of the method. A series of Ln-bdc compounds were synthesized by reacting Ln^{3+} salts with H_2bdc in e-urea semihydrate solvent at 140 °C. Topologically, these new Ln-bdc phases are either isostructural to the Y^{3+} compound **1** (**1a**–**g**; Supporting Information, Table S1) or **2** (**2a**–**c**), and Sm(bdc)$_{3/2}$(e-urea) obtained from deep eutectic solvents (**9**, **9a**–**b**),[6h] or exhibit new crystalline structures (**20**–**30**, see the Supporting Information, Table S1 for details). Furthermore, reactions of d-block metal ions (including Group 12 ions) with bdc also yielded a number of new phases (**40**–**45**, Tables 1; Supporting Information, S1). For example, the assembly of Co^{2+} or Cd^{2+} with bdc in tm-urea generated two 3D open-frameworks (URO-44 and URO-45) with 1D channels (Figure 2 c,d). In both frameworks, the tm-urea solvent molecules are located within the channels and serve as the templates (as compared to pendent ligands in **1**–**9**).

So far we have used the bdc ligand exclusively to focus on roles of different urea derivatives. Clearly, the urothermal synthesis works with other crosslinking ligands as well (Supporting Information, Scheme S1, Table S1). Three notable examples are URO-123, URO-160, and Zn/BTB-tsx-pyrol (BTB = 1,3,5-benzenetribenzoate). URO-123 based on 1,2,4-benzenetricarboxylate and Zn^{2+} possesses a chiral microporous framework with large rectangular channels along the *a* axis (Figure 2 b), while URO-160 constructed from thio-

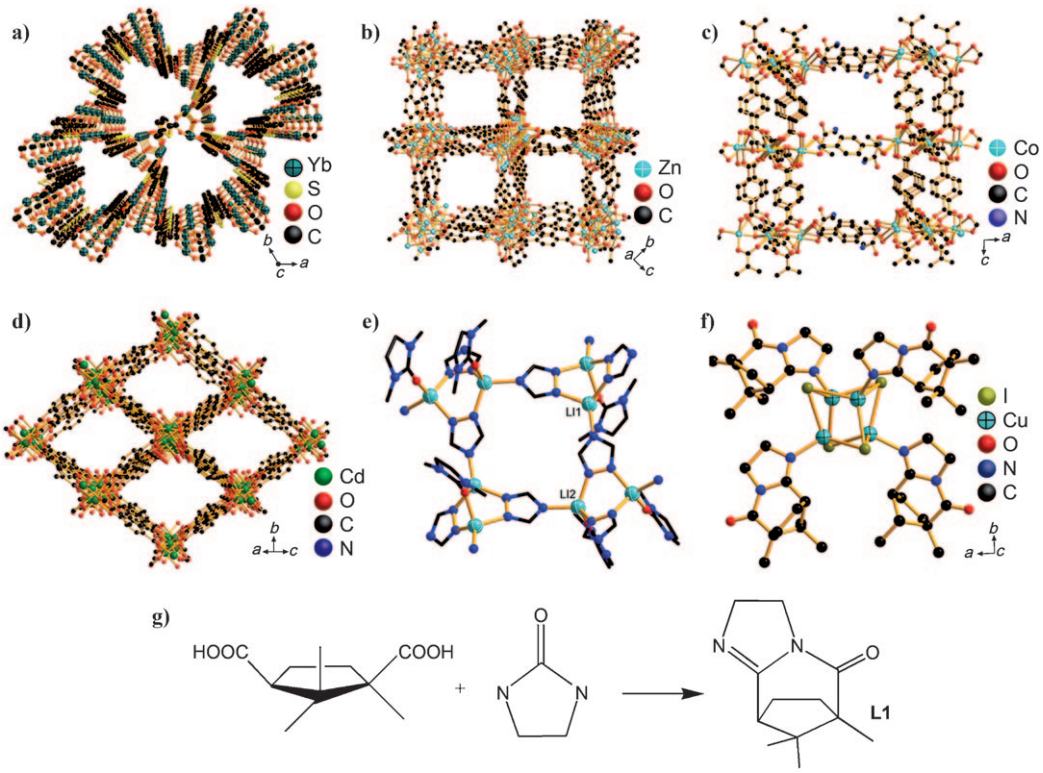

Figure 2. a–d) The 3D frameworks of a) URO-160, b) URO-123, c) URO-44, and d) URO-45. e) The coordination environment in URO-511, f) the molecular structure of URO-502, and g) representation of the in situ synthesis of the enantiopure **L1** ligand in URO-502.

phene-2,5-dicarboxylate is a nitrate anion templated porous framework with exposed Yb_3O trimeric units (Figure 2a). In Zn/BTB-tsx-pyrol, which is related to Zn/BTB-tsx,[1g] an interesting feature is that there are two pyrol ligands attached to each Zn_4O unit. Furthermore, previously reported highly porous materials can also be made. For example, U-MOF-177 (Supporting Information, Table S1) has been made by using p-murea/H_2O as the solvent, instead of DEF originally used for synthesizing MOF-177.[1b]

Frameworks consisting of Li^+ ions are quite rare, in part because of the high solvation energy of Li^+. Thus it is of particular interest to develop new solvent systems for making lithium frameworks. As an example of the relevance of the urothermal synthesis to the preparation of lithium framework structures, URO-511 was synthesized by using e-murea (Figure 2e).

A particularly interesting finding is the reaction of D-camphoric acid with ethyleneurea to generate a new enantiopure ligand (L1) found in URO-502 (Figure 2f,g), thus demonstrating that the versatility of the urothermal method extends beyond the synthesis of crystalline porous materials to include unusual organic transformations.

Thermal gravimetric analysis indicates that Y-bdc compounds (**1**–**4**, **6**, **8**) exhibit a sharp weight loss upon solvent removal between 200–300 °C and remain stable up to about 500 °C (Supporting Information, Figure S11). After heating **2** to **4** at 250 °C for 10 min, powder X-ray diffraction shows that samples **2** to **4** have the same pattern before and after the heating, confirming that they are stable towards the solvent loss (Supporting Information, Figure S14). Volumetric gas adsorption measurements (N_2, H_2, and CO_2) for select samples were also performed. The samples of **1**, **2**, **6**, and URO-123 were degassed at 200 °C prior to the measurement. The N_2 adsorption/desorption studies of **1**, **2**, **6**, and URO-123 reveal that all of them are porous (Supporting Information, Figures S11–S13). BET and Langmuir surface areas for each sample are summarized in the Supporting Information, Table S2, together with the H_2 adsorption results at 77 K and 1 atm and the CO_2 adsorption results at 273 K and 1 atm. The porosity values shown by these materials (Langmuir surface areas from 198 to 300 $cm^3 g^{-1}$) demonstrate that the promise of urothermal synthesis goes beyond just the creation of diverse structural types to include the generation of porosity.

In conclusion, we have demonstrated that urothermal synthesis, based on the use of urea derivatives as solvents, offer promise for the synthesis of a wide range of crystalline materials. In particular, we show that the method is well suited for the creation of crystalline porous materials through the reversible binding of urea-type ligands to framework metal sites. It is expected that further refinement of urothermal method will have a great potential for the creation of novel porous materials with promising applications.

Received: June 27, 2010
Revised: August 18, 2010
Published online: October 15, 2010

Keywords: metal–organic frameworks · microporous materials · solvent effects · solvothermal synthesis · urea

[1] a) A. K. Cheetham, G. Ferey, T. Loiseau, *Angew. Chem.* **1999**, *111*, 3466; *Angew. Chem. Int. Ed.* **1999**, *38*, 3268; b) H. K. Chae, D. Y. Siberio-Perez, J. Kim, Y. Go, M. Eddaoudi, A. J. Matzger, M. O'Keeffe, O. M. Yaghi, *Nature* **2004**, *427*, 523; c) G. Férey, *Chem. Soc. Rev.* **2008**, *37*, 191; d) S. Horike, S. Shimomura, S. Kitagawa, *Nat. Chem.* **2009**, *1*, 695; e) B. Chen, S. Xiang, G. Qian, *Acc. Chem. Res.* **2010**, *43*, 1115; f) C. Serre, C. Mellot-Draznieks, S. Surble, N. Audebrand, Y. Fillinchuk, G. Ferey, *Science* **2007**, *315*, 1828; g) S. R. Caskey, A. G. Wong-Foy, A. J. Matzger, *Inorg. Chem.* **2008**, *47*, 7751.

[2] a) R. E. Morris, P. S. Wheatley, *Angew. Chem.* **2008**, *120*, 5044; *Angew. Chem. Int. Ed.* **2008**, *47*, 4966; b) L. J. Murray, M. Dinca, J. R. Long, *Chem. Soc. Rev.* **2009**, *38*, 1294; c) S. Ma, H. Zhou, *Chem. Commun.* **2010**, *46*, 44; d) L. Pan, M. B. Sander, X. Huang, J. Li, M. Smith, E. Bittner, B. Bockrath, J. K. Johnson, *J. Am. Chem. Soc.* **2004**, *126*, 1308.

[3] a) A. R. Millward, O. M. Yaghi, *J. Am. Chem. Soc.* **2005**, *127*, 17998; b) R. Banerjee, A. Phan, B. Wang, C. Knobler, H. Furukawa, M. O'Keeffe, O. M. Yaghi, *Science* **2008**, *319*, 939.

[4] a) D. Bradshaw, J. B. Claridge, E. J. Cussen, T. J. Prior, M. J. Rosseinsky, *Acc. Chem. Res.* **2005**, *38*, 273; b) L. Ma, C. Abney, W. Lin, *Chem. Soc. Rev.* **2009**, *38*, 1248; c) J. Y. Lee, O. K. Farha, J. Roberts, K. A. Scheidt, S. T. Nguyen, J. T. Hupp, *Chem. Soc. Rev.* **2009**, *38*, 1450.

[5] R. E. Morris, S. J. Weigel, *Chem. Soc. Rev.* **1997**, *26*, 309.

[6] a) K. Jin, X. Huang, L. Pan, J. Li, A. Appel, S. Wherland, *Chem. Commun.* **2002**, 2872; b) E. R. Cooper, C. D. Andrews, P. S. Wheatley, P. B. Webb, P. Wormald, R. E. Morris, *Nature* **2004**, *430*, 1012; c) R. E. Morris, *Chem. Commun.* **2009**, 2990; d) E. R. Parnham, R. E. Morris, *Acc. Chem. Res.* **2007**, *40*, 1005; e) J. Zhang, S. Chen, X. Bu, *Angew. Chem.* **2008**, *120*, 5514; *Angew. Chem. Int. Ed.* **2008**, *47*, 5434; f) P. C. Jhang, Y. C. Yang, Y. C. Lai, W. R. Liu, S. L. Wang, *Angew. Chem.* **2009**, *121*, 756; *Angew. Chem. Int. Ed.* **2009**, *48*, 742; g) M. F. Tang, Y. H. Liu, P. C. Chang, Y. C. Liao, H. M. Kao, K. H. Lii, *Dalton Trans.* **2007**, 4523; h) J. Zhang, T. Wu, S. Chen, P. Feng, X. Bu, *Angew. Chem.* **2009**, *121*, 3538; *Angew. Chem. Int. Ed.* **2009**, *48*, 3486.

